Engineering Analysis with Boundary Elements 161 (2024) 179–187

Contents lists available at ScienceDirect

Engineering Analysis with Boundary Elements

journal homepage: www.elsevier.com/locate/enganabound

Effect of polycaprolactone percentage on thermal and mechanical behavior of polyurethane/polycaprolactone/graphene oxide nanocomposite utilizing molecular dynamics simulation

Shapour Fadaei Heydari, Mohamad Shahgholi *, Mehdi Salehi, Seyed Ali Galehdari

Department of Mechanical Engineering, Najafabad Branch, Islamic Azad University, Najafabad, Iran

ARTICLE INFO

Keywords:
Polycaprolactone
Nanocomposite
LAMMPS
Heat Flux
Ultimate Strength
Mean Square Displacement

ABSTRACT

Shape memory polymers belong to a category of smart materials capable of changing their predetermined shape in response to specific stimuli like temperature, electricity, or magnetic fields. Polycaprolactone is an example of a biodegradable polyester from the aliphatic polyester family that has been extensively studied due to its unique mechanical properties, compatibility with various polymers, and biodegradability. In this upcoming research, different amounts of polycaprolactone have been added to investigate its impact on the thermal-mechanical behavior of a smart polymer nanocomposite consisting of polyurethane/polycaprolactone/graphene oxide. The thermal, mechanical, and atomic properties of this designed nanocomposite have been evaluated utilizing molecular dynamics simulation technique and LAMMPS software. The findings of the research illustrated that by increasing the amount of polycaprolactone from 10 to 50%, the heat flux and thermal conductivity in the modeled nanocomposite increased from 688.43 to 724.03 W/m^2 and from 0.85 to 0.99 W/m.K. Also, increasing the amount of polycaprolactone from 10 to 50% has led to an increase in the ultimate strength and Young's modulus of the studied nanocomposite from 56.32 to 62.23 MPa and from 5.99 to 6.29 MPa. The mean square displacement parameter and glass transition temperature have converged to 0.31 Å^2 and 331 K with increasing amount of polycaprolactone.

1. Introduction

Intelligence in materials is a characteristic that is not limited to a specific group and is observed in most groups of materials. Polymers are no exception to this phenomenon and exhibit different responses to various stimuli such as temperature (temp), pressure (press), electric fields, and magnetic fields. These polymers are categorized into different groups with distinct properties and applications [1–3]. Among the well-known branches of smart polymers that have gained widespread commercial use, we can mention shape memory polymers, electroactive polymers, self-healing polymers, and polymers carrying phase change materials. These types of polymers are further classified into three categories based on the type of stimulus they respond to: physical stimuli, chemical stimuli, and biological stimuli [4–7]. Shape memory polymers belong to a class of smart materials that can change their predetermined shape when exposed to certain stimuli like temp, electricity, or magnetic fields. These polymers have been proposed since 1981 and come in various types [8]. Similar to regular polymers, shape memory polymers have a lattice-like three-dimensional molecular structure consisting of "fixing points" and polymer segments connecting these points are called transfer phase [9]. Among the different types of shape memory polymers sensitive to the mentioned stimuli, thermal shape memory polymers have received more attention. Polycaprolactone (PCL) is an example of a biodegradable polyester belonging to the aliphatic polyester family. It is produced through the ring-opening polymerization of caprolactone (CL) monomers. This material has been extensively studied due to its unique mechanical properties, compatibility with various other polymers, and biodegradability [10–12]. The composite polymer's physical, mechanical, and thermal properties are influenced by its molecular weight and transparency value, which affects its degradability through hydrolysis of ester bonds in physiological conditions. PCL is highly hydrophobic, has a semi-crystalline state, and easily dissolves at room temp. Its low melting point and high compositional compatibility make it easy to process. These properties have motivated researchers to explore the potential use of PCL in biobiology [13–15].

Nowadays, various methods for characterization of materials are

* Corresponding author.
E-mail address: m.shahgholi@pmc.iaun.ac.ir (M. Shahgholi).

https://doi.org/10.1016/j.enganabound.2024.01.014
Received 15 July 2023; Received in revised form 1 January 2024; Accepted 17 January 2024
Available online 1 February 2024

used like numerical estimation of characteristics [16], finite element methods [17], different computer based modeling [18], Simulation based on molecular activities [19] and the studies based on the experiments [20]. Material reinforcement by utilizing NPs is under attention to improve properties of the materials or even nanofluids [21–23].

Babaei et al. [24] conducted a study to examine the impact of molecular weight variations in shape memory polyurethanes (SMPUs) and graphene content on the mechanical properties and shape memory behavior of polyurethane (PU)/graphene nanocomposites (NCs). The findings revealed that changes in the molecular weight of the PCL component and graphene nanosheet concentration influenced the transition and crystallization temperatures of the samples. Additionally, the presence of nanosheets restricted the mobility of PCL chains, resulting in a higher shape constant ratio. Moreover, the nanoplates prevented stress transfer to the hard parts, leading to an increased shape recovery ratio. In another study, Boudjellal et al. [25] synthesized and examined the mechanical properties of a composite consisting of alpha fibers and graphene/PCL nanoplatelets. The results demonstrated that incorporating 5% by weight of graphene nanoplatelets enhanced the tensile strength of PCL from 13.23 to 14.18 MPa, as well as increased Young's modulus (YM) from 248.75 to 431.15 MPa. Stefanovic et al. [26] investigated the influence of adding PCL on the thermal and mechanical properties of PU. The findings indicated that incorporating PCL significantly improved these properties; however, it resulted in a decrease in crosslink density and hydrogen bond formation potential. Shahsavari et al. [27] explored the shape memory behavior of PCL/thermoplastic starch/graphene nanoplatelet NCs. The results revealed that different stimuli had varying effects on the composite's shape memory behavior. Notably, utilizing water as a propellant improved shape recovery by reducing the weight percentage of PCL from 30% to 10%. Wang et al. [28] investigated the thermal and mechanical properties of thermoplastic PU in their study. The findings of the study revealed that when the smart polymer is exposed to light stimulus such as infrared rays and direct sunlight, it becomes activated. Additionally, the light radiation enhances the strength of the surface bond, thereby improving the mechanical properties of the product. Cetiner et al. [29] conducted a study to examine how adding thermoplastic PU and graphene nanoplatelets to polylactic acid affects its shape, mechanical, and thermal memory behavior. The results indicated that incorporating PU into polylactic acid at a weight ratio of 9:1 improves flexibility and shape memory behavior. Furthermore, adding 0.5% by weight of graphene nanoplatelets increases mechanical properties by 24% and thermal properties by 15%. Liang et al. [30] investigated the impact of adding graphene oxide (GO)-nanoparticles (NPs) on the mechanical properties of PU. The findings demonstrated that incorporating 0.70% by weight of graphene NPs increases the tensile strength of the NC by 64.89%.

Based on the studies conducted in this field, it can be concluded that a comprehensive study on the shape memory, mechanical and thermal properties of smart polymer NCs of PU/PCL/ GO has not been done by the molecular dynamics (MD) simulation. Therefore, in this study, the effects of different percentages of PCL (10, 20, 30 and 50%) on the shape memory, mechanical and thermal properties of smart polymer NC PU/ PCL/ GO are focused. In this research, various polymer structures have been modeled utilizing Avogadro software, and the balance of the structure, properties such as heat flux (HF), thermal conductivity (TC), final volume, ultimate strength (US), YM, mean square displacement (MSD) and glass transition temp (T_g) in a period of 10 ns has been evaluated and reported. The MD simulations in nanodimensions are a suitable and useful method in the present research, and as a result, the outputs of these simulations can be utilized in practical fields.

2. Simulation method

Currently, scientists have been researching the shape memory properties of various polymers, particularly engineering polymers and biopolymers, in order to develop materials with shape memory capabilities as well as mechanical properties and biocompatibility. This study focuses on enhancing the properties of PCL, a biocompatible polymer derived from natural sources, by incorporating it into a smart polymer NC made of PU and GO- NPs. The impact of adding PCL is evaluated through computer simulations, specifically MD simulation. To examine the effect on the thermal-mechanical behavior of the NC, different amounts of PCL (10, 20, 30, and 50%) are considered. The simulations are conducted in a cubic chamber measuring 300 nm. The modeling process involves utilizing Avogadro software to create structures for the polymers and NPs, which are then assembled in a simulation box utilizing Packmol software. The thermal and mechanical properties of the simulated NC are assessed utilizing LAMMPS computing software. To ensure structural balance, the NVT ensemble at a temp of 300 K is employed. Physical values such as temp and PE are calculated for the structure under investigation. The time required to check the balance is considered to be 10 ns and sampling occurring every 20,000 time steps. The total simulation time is 20 ns with a time step of 1 fs. Temp and press adjustments are made utilizing Langevin thermostat and Brandsen barostat respectively. Fig. 1 displays the atomic structure of the simulated samples with varying amounts of PCL.

3. Results and discussion

In this section, the results of MD simulation and LAMMPS software for the modeled NC are reported. In the first step of the present MD simulations, the thermodynamic equilibrium in the samples has been examined by examining the temporal changes of physical quantities including temp and PE. The ensemble utilized to check the balance is NVT and the required time is considered to be 10 ns. To verify the thermodynamic equilibrium in the simulated sample, the initial temp of the structure is set to 300 K. Fig. 2 illustrates the temp variations across the entire atomic sample over time during the simulation. The obtained results indicate that during the initial stages of the simulation, there are temp fluctuations that signify the mobility and fluctuations of NPs within the simulated structure. However, as the simulation time increases to 10 ns, the temp within the sample converges to 300 K, indicating that the atomic structure has reached thermodynamic equilibrium. From a physical standpoint, this temp balance in the samples suggests that there is no divergence in fluctuation range among structures within the simulation box, thus indicating stability. This thermodynamic behavior demonstrates a reduction in temp fluctuations over time, which further confirms stability in atomic samples. Moreover, despite achieving thermodynamic equilibrium in the simulation sample, it can be concluded that MD simulations yield reliable results. Additionally, the temp balance observed in the atomic sample validates that a simulation time of 10 ns is sufficient for this research.

To ensure that the simulated samples are thermodynamically balanced at a temp of 300 K, the PE of the atomic structures is calculated. Fig. 3 presents the results of this calculation, showing that the numerical value of the PE converges to 16.77 kcal/mol after 10 ns. A negative value indicates interatomic attraction in the structures, while convergence suggests stability in the positions of the atoms. This indicates that the proposed atomic sample is physically stable for practical applications.

After balancing, the thermal-mechanical behavior of the simulated sample is evaluated utilizing the NPT ensemble within the simulation box. HF, TC, and volume change are calculated to assess the thermal behavior. To study how adding PCL affects this behavior in a designed NC, different amounts (10, 20, 30, and 50%) are considered and simulations are repeated. Fig. 4 illustrates changes in HF for a PU/PCL/ GO NC sample at a temp of 300 K and press of 1 bar based on varying amounts of PCL. Analysis of HF and conductivity coefficient reveals improved thermal behavior when adding PCL to the target NC structure. From a numerical perspective, when the amount of PCL is increased from 10 to 50%, the HF in the structures increases from 688.43 to 724.03

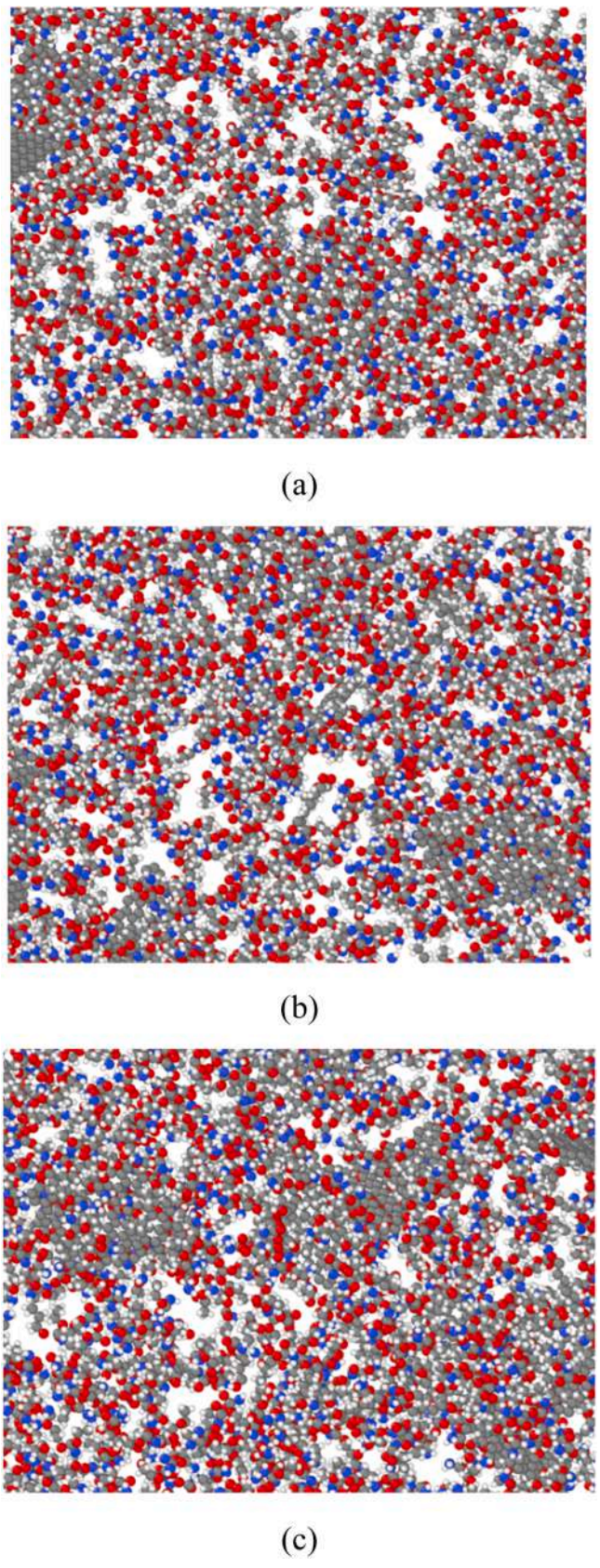

Fig. 1. Atomic structure modeled during the equilibration process for NC with the presence of a) 20, b) 30 and c) 50% PCL.

W/m^2. On an atomic level, this occurs due to intensified interatomic collisions and increased particle oscillations within the structure, resulting in improved heat transfer within the simulation box.

Fig. 5, illustrates the changes in TC coefficient in the PU/PCL/ GO NC sample at a temp of 300 K and press of 1 bar, based on the amount of PCL present. The TC coefficient indicates a material's ability to transfer heat, with higher coefficients indicating greater heat transfer to larger surfaces and at higher speeds. The results of MD simulation demonstrate an increase in the TC coefficient when the amount of PCL is increased from 10% to 50%, rising from 0.85 W/m.K to 0.99 W/m.K. Consequently, the increase in HF leads to an increase in the TC coefficient as more heat is generated due to enhanced particle mobility and fluctuations within the structure. Additionally, in the modeled NC, increasing the amount of PCL results in more collisions and stronger attraction between particles, leading to increased adhesion between the base matrix and added NPs (PU and GO). This ultimately contributes to an increase in the TC coefficient of the studied NC.

Fig. 6, illustrates the changes in volume of a NC sample made of PU, PCL, and GO at a temp of 300 K and a press of 1 bar, based on the amount of PCL present. This analysis allows us to predict the structural stability and mechanical usability of the sample. The numerical data shows that increasing the amount of PCL from 10% to 50% results in a convergence of the sample's volume from 27311 to 27913 nm^3, indicating structural stability.

Fig. 7, displays the changes in stress-strain behavior in the NC sample as more PCL is added. The stress-strain diagram demonstrates an increase in US and overall strength due to the addition of PCL. This can be attributed to an increase in particle collisions and fluctuations within the matrix, resulting in more bonding and ultimately enhancing the structure's US. Based on Fig. 7 and the numerical results obtained, it is observed that US occurs at a strain of 950%. In samples containing 10%, 20%, 30%, and 50% PCL, the corresponding US values are measured as 56.32, 58.14, 59.15, and 62.23 MPa respectively.

In this step, the US and YM values of the samples are reported based on the amount of PCL, as shown in Fig. 8. The results of the MD simulation indicate that adding PCL increases the US and resistance of the NC. Increasing the amount of PCL from 10% to 50% leads to an increase in the US from 56.32 to 62.23 MPa. This is because more particles in the matrix result in more collisions and fluctuations, leading to more bonds and increased strength. Therefore, the amount of PCL should be considered in thermal and mechanical applications of these samples.

Fig.9, illustrates the changes in YM in the NC sample as the amount of PCL increases. According to this figure, increasing the percentage of PCL from 10% to 50% leads to an increase in YM from 5.99 to 6.29 MPa, indicating an enhancement in the US of the NC. This can be attributed to an increase in particle collisions and oscillations within the matrix, resulting in stronger attraction between composite particles. These factors contribute to an overall increase in US and YM.

Finally, in order to check the T_g in the simulated samples, the temp is changed in the sample and the temp related to the phase change of the final structure is measured. Based on the results presented in Table 1, with the increase in the amount of PCL, the T_g in the sample increases, and this high T_g increases the MSD parameter according to Fig. 10 The MSD parameter usually increases with increasing T_g due to increased mobility of molecules or particles in the material. This increased mobility allows the molecules or particles to move more freely, resulting in larger displacements and higher MSD values. The numerical findings demonstrate that by increasing the proportion of PCL to 50%, the MSD and T_g of the sample converge to 0.31 $Å^2$ and 331 K, respectively. These results suggest that this composition could be suitable for thermal applications.

The results obtained from the simulations conducted in this study are presented in Table 1, which includes information on the atomic, thermal, and mechanical properties of the PU/PCL/GO NC. The simulations were performed at a temp of 300 K and a press of 1 bar, with varying amounts of PCL.

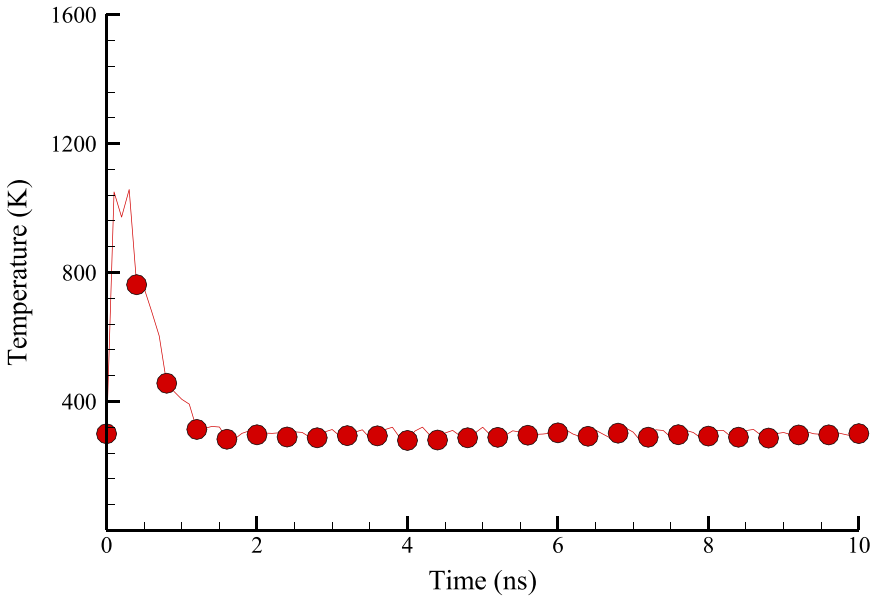

Fig. 2. Temp changes in the studied sample according to simulation time.

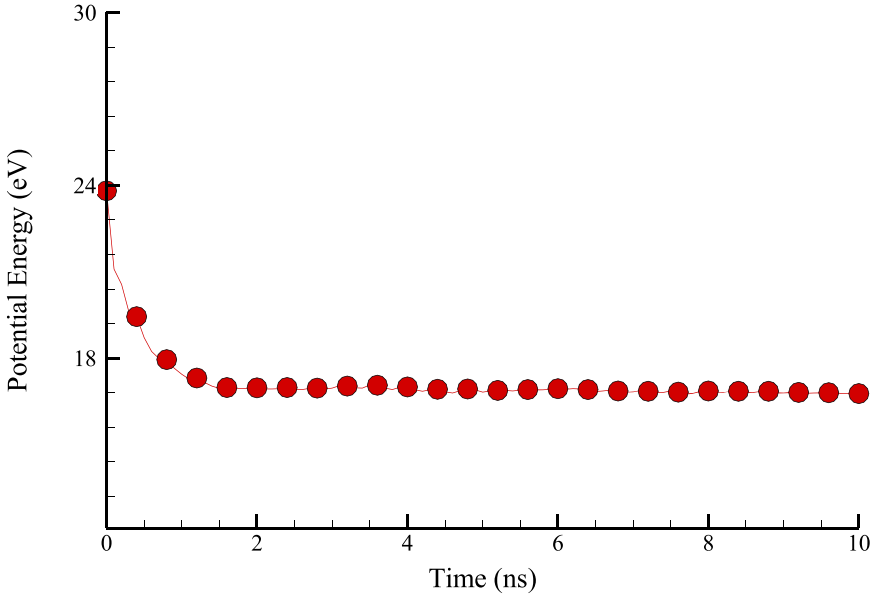

Fig. 3. PE changes in the studied sample according to simulation time.

4. Conclusion

The study utilized the MD method and LAMMPS computing software to examine the thermal and mechanical properties of the PU/PCL/GO NC. The simulation results were divided into two parts: the equilibration of the NC over a 10 ns period, where temp and potential energy (PE) were assessed, and the investigation of the mechanical and thermal behavior of the NC with varying amounts of PCL. The results from the atomic samples indicated that:

- The designed NC reached a temp of 300 K after 10 ns, suggesting a reduction in temp fluctuations and particle mobility, resulting in a balanced and stable structure.
- Numerically, the PE in the designed NC converged to 16.77 kcal/mol, indicating an average attractive force between particles in different regions of the simulation box.

After observing equilibrium in the atomic samples, further analysis on the thermal and mechanical behavior was conducted, yielding the following findings:

- Numerically, as PCL content increased from 10% to 50%, HF in the structures increased from 688.43 to 724.03 W/m^2.
- With an increase in PCL content, there was an increase in collisions and attraction between particles, leading to stronger adhesion between the base matrix and NPs, ultimately resulting in a higher TC.
- Increasing PCL content from 10% to 50% resulted in an increase in TC from 0.85 to 0.99 W/m.K.
- Increasing PCL content from 10% to 50% led to an increase in US of the modeled NC from 56.32 to 62.23 MPa.
- An increase in particle count within the matrix led to more collisions and fluctuations, resulting in more bonds being formed and ultimately increasing US of the structure.

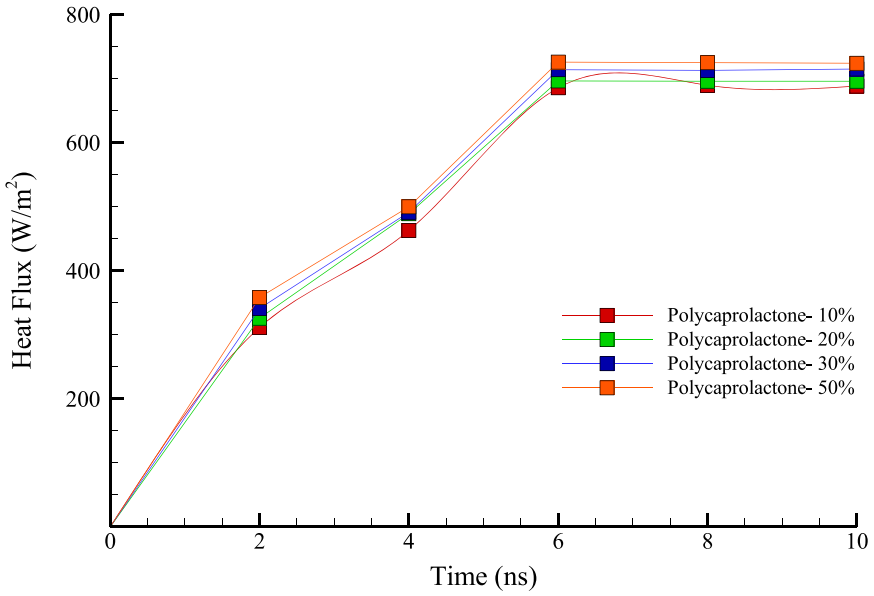

Fig. 4. Changes in the HF of the designed NC according to the amount of PCL.

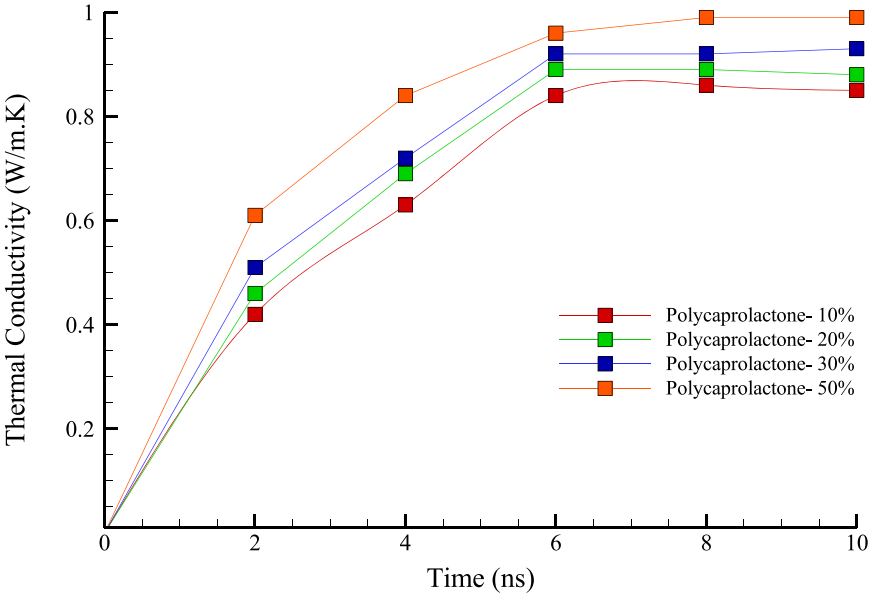

Fig. 5. Changes in the TC of the designed NC according to the amount of PCL.

CRediT authorship contribution statement

Shapour Fadaei Heydari: Conceptualization, Data curation, Software. **Mohamad Shahgholi:** Project administration, Writing – review & editing. **Mehdi Salehi:** Formal analysis, Validation. **Seyed Ali Galehdari:** Conceptualization, Validation, Visualization.

Declaration of competing interest

The authors declare that they have no known competing financial interests or personal relationships that could have appeared to influence the work reported in this paper.

Data availability

Data will be made available on request.

Appendix

The MD simulation is a computer-based method that has been expanded and developed to study the behavior and properties of particles and materials at the atomic level. This approach involves simulating the movement and interactions of individual atoms or particles over a certain period

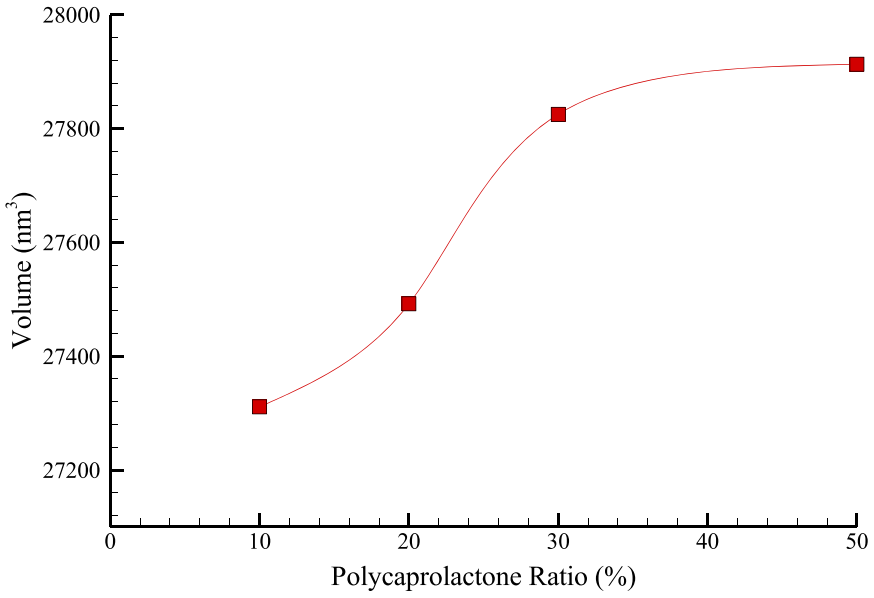

Fig. 6. Volume changes of the designed NC according to the amount of PCL.

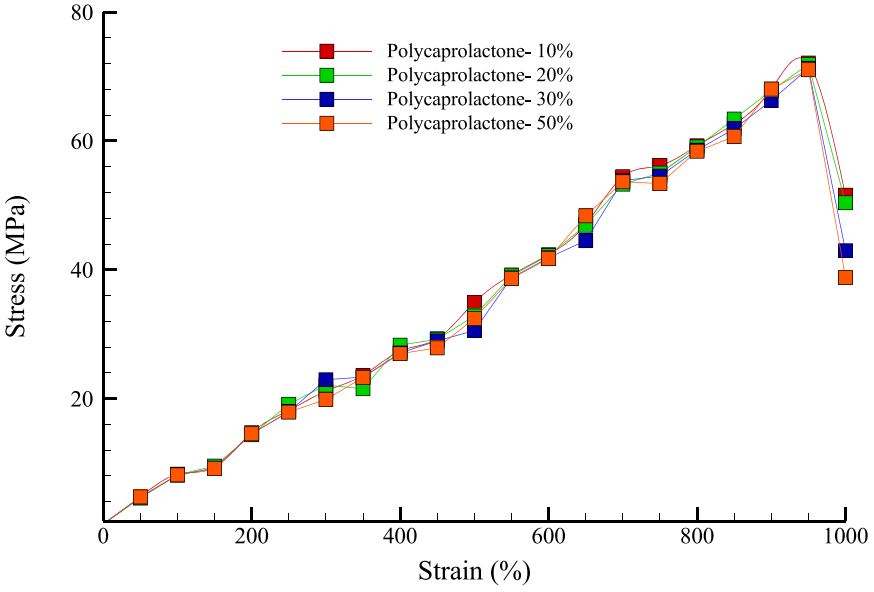

Fig. 7. Variations of the stress-strain diagram in the designed NC according to the amount of PCL.

of time, providing insights into various physical, chemical, and biological phenomena. MD simulations are particularly useful for predicting system behavior under conditions that are difficult to access experimentally, such as extreme temps or press. Consequently, this method has become an important tool for designing and optimizing materials with unique properties [31–34]. LAMMPS is a widely utilized software package for conducting MD simulations. It is specifically designed to efficiently simulate large-scale systems containing millions or even billions of particles. The software offers a wide range of force fields and simulation techniques, making it versatile for various research fields [35,36]. The fundamental principle of MD simulation involves solving equations and Newton's second law for individual particles. Newton's second equation establishes the relationship between force, mass, and particle acceleration [37]:

$$F_i = \sum_{i \neq j} F_{ij} = m_i \frac{d^2 r_i}{dt^2} = m_i \frac{dv_i}{dt} \tag{1}$$

To initiate a MD simulation, the first step is to define the desired system by specifying the types and quantities of particles, their initial positions and velocities, as well as any constraints or boundary conditions. The subsequent step involves selecting an appropriate force field for the particles and system under study. A force field is a mathematical model that describes how particles interact within a system. It comprises two main components: bonding and non-bonding interactions. The choice of force field depends on the nature of the system and the desired level of accuracy. In each time step, forces acting on each particle are calculated based on the chosen force field [36,38,39]. These forces are derived from the gradient of the potential energy (PE) function relative to particle positions [37]:

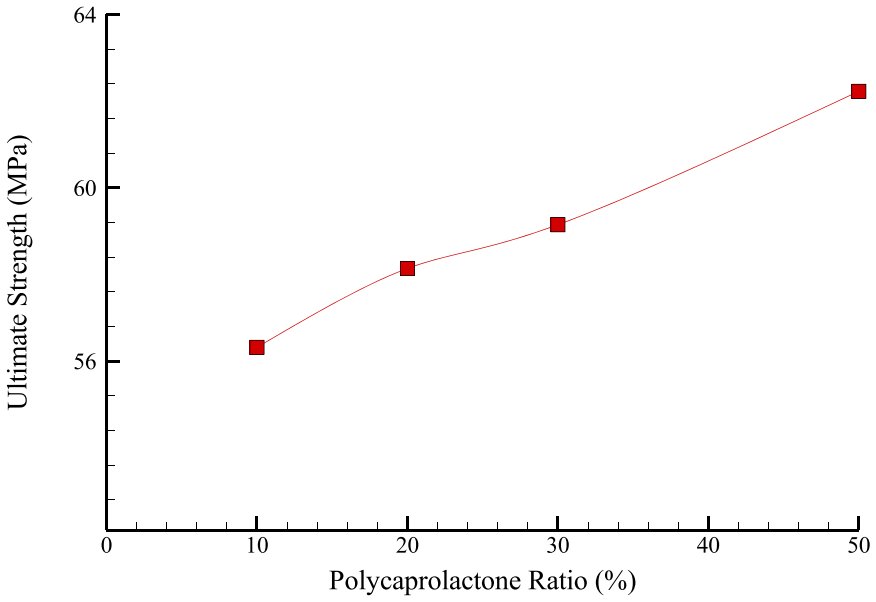

Fig. 8. US changes in the designed NC according to the amount of PCL.

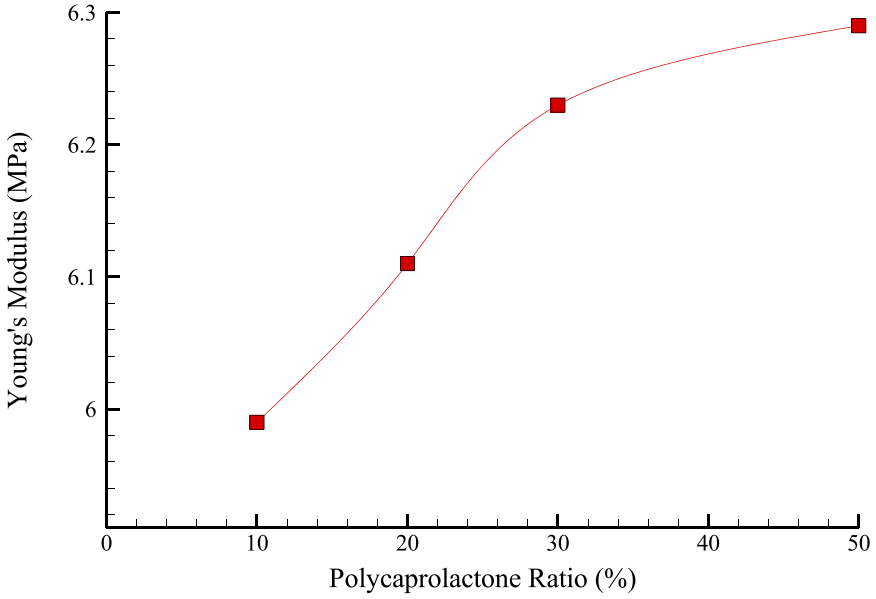

Fig. 9. Changes of YM in designed NC according to the amount of PCL.

Table 1
Atomic, thermal and mechanical outputs of the simulated NC according to the amount of PCL.

PCL (%)	HF (W/m^2)	TC (W/m.K)	Final Volume (nm^3)	US (MPa)	YM (MPa)	MSD (Å^2)	T_g (K)
10	688.43	0.85	27311	56.32	5.99	0.25	321
20	695.94	0.88	27492	58.14	6.11	0.26	324
30	714.93	0.93	27825	59.15	6.23	0.28	328
50	724.03	0.99	27913	62.23	6.29	0.31	331

$$F_i = -\nabla U_i = -\frac{\partial U}{\partial r_i} \tag{2}$$

In our upcoming research, we have employed the Lennard-Jones (LJ) and Coulomb potential function to investigate non-bonded interactions. The LJ potential accounts for van der Waals interactions between atoms and is characterized by two parameters: the strength of interaction represented by

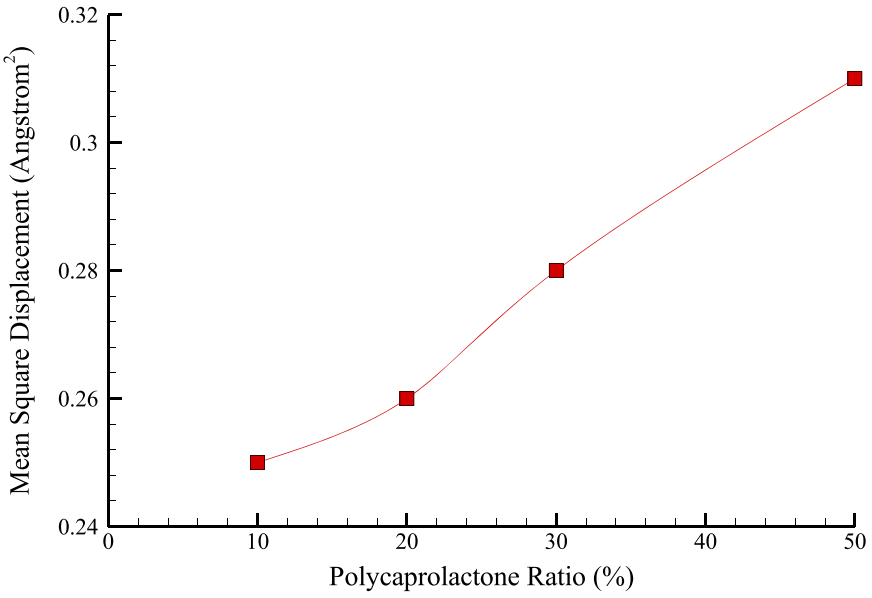

Fig. 10. Variations of the MSD in the designed NC sample according to the amount of PCL.

the size of the potential well (ε_{ij}), and the equilibrium distance where PE is zero (σ_{ij}) [40,41] (See Table A):

$$U_{LJ} = 4\varepsilon_{ij}\left[\left(\frac{\sigma_{ij}}{r}\right)^{12} - \left(\frac{\sigma_{ij}}{r}\right)^{6}\right] \tag{3}$$

Table A
LJ potential function parameters of the present particles [42,43]

Particles	ε (kcal/mol)	σ (Å)
H	0.01	3.20
O	0.415	3.71
C	0.3050	4.18
N	0.415	3.995

The values of σ and ε of each interaction between the particles were calculated utilizing Eqs. (3) and (4) [42]:

$$\varepsilon_{ij} = \sqrt{\varepsilon_i \varepsilon_j} \tag{4}$$

$$\sigma_{ij} = \frac{\sigma_i + \sigma_j}{2} \tag{5}$$

As stated earlier, the potential function utilized to determine the electrostatic forces between charged particles is the Coulomb potential function and is expressed by the following equation [44]:

$$U_{ij}(r) = \frac{-1}{4\pi\varepsilon_0}\frac{q_i q_j}{r_{ij}^2} \tag{6}$$

Once both the system and force field are defined, we proceed to solve equations of motion for each particle. However, due to a large number of particles involved, it is not feasible to analytically solve equations of motion individually for each particle as it leads to numerous errors. Therefore, numerical solution methods must be employed to integrate equations of motion for each particle in order to simulate their behavior over time. The most common integration algorithm is the Verlet – velocity algorithm, which is based on the Taylor series expansion. Based on this type of algorithm, the position $r_i(t)$ and velocity $v_i(t)$of the particles are calculated in each time step (t), and then in the next time steps ($t + \delta t$), utilizing the mentioned values, the new velocity $v_i(t + \delta t)$ and position $r_i(t + \delta t)$of the particles are calculated. The formulation of this type of algorithm is as follows [45,46]:

$$r_i(t + \Delta t) = r_i(t) + \Delta t\ v_i(t) + \frac{\Delta t^2 a_i\ (t)}{2} \tag{7}$$

$$v_i(t + \Delta t) = v_i(t) + \Delta t\ a_i(t) + \frac{\Delta t\ (a_i\ (t) + a_i(t + \Delta t))}{2} \tag{8}$$

References

[1] H. Palza, P.A. Zapata, and C. Angulo-Pineda, "Electroactive smart polymers for biomedical applications," vol. 12, no. 2, p. 277, 2019.
[2] B. Gong et al., "Magnetic field-responsive smart polymer composites," pp. 137–89, 2007.
[3] L. Jingcheng, V.S. Reddy, W.A. Jayathilaka, A. Chinnappan, S. Ramakrishna, and R. Ghosh, "Intelligent polymers, fibers and applications," vol. 13, no. 9, p. 1427, 2021.
[4] K. Strzelec, N. Sienkiewicz, and T. Szmechtyk, "Classification of shape-memory polymers, polymer blends, and composites," pp. 21–52, 2020.
[5] D. Ratna and J. Karger-Kocsis, "Recent advances in shape memory polymers and composites: a review," vol. 43, pp. 254–69, 2008.
[6] J. Hu, Y. Zhu, H. Huang, and J. Lu, "Recent advances in shape–memory polymers: structure, mechanism, functionality, modeling and applications," vol. 37, no. 12, pp. 1720–63, 2012.
[7] Amreen K, Goel S. Smart polymers in flexible devices. Specialty polymers. CRC Press; 2023. p. 459–72.
[8] B.I. Oladapo, J.F. Kayode, J.O. Akinyoola, and O.M. Ikumapayi, "Shape memory polymer review for flexible artificial intelligence materials of biomedical," vol. 293, p. 126930, 2023.
[9] C. Liu, H. Qin, and P. Mather, "Review of progress in shape-memory polymers," vol. 17, no. 16, pp. 1543–58, 2007.
[10] Fakirov S. Biodegradable polyesters. John Wiley & Sons; 2015.
[11] E. Archer, M. Torretti, and S. Madbouly, "Biodegradable polycaprolactone (PCL) based polymer and composites," no. 0, p. 000010151520200074, 2021.
[12] I. Armentano, M. Gigli, F. Morena, C. Argentati, L. Torre, and S. Martino, "Recent advances in nanocomposites based on aliphatic polyesters: design, synthesis, and applications in regenerative medicine," vol. 8, no. 9, p. 1452, 2018.
[13] R. Dwivedi et al., "Polycaprolactone as biomaterial for bone scaffolds: review of literature," vol. 10, no. 1, pp. 381–8, 2020.
[14] M. Abedalwafa, F. Wang, L. Wang, and C. Li, "Biodegradable poly-epsilon-caprolactone (PCL) for tissue engineering applications: a review," vol. 34, no. 2, pp. 123–40, 2013.
[15] S.H. Chang, H.J. Lee, S. Park, Y. Kim, and B. Jeong, "Fast degradable polycaprolactone for drug delivery," vol. 19, no. 6, pp. 2302–7, 2018.
[16] Salimpour MR, Karimi Darvanjooghi MH, Abdollahi A, Karimipour A, Goodarzi M. Providing a model for Csf according to pool boiling convection heat transfer of water/ferrous oxide nanofluid using sensitivity analysis. Int J Numer Methods Heat Fluid Flow 2020;30(6):2867–81.
[17] Fada R, Shahgholi M, Azimi R, et al. Estimation of porosity effect on mechanical properties in calcium phosphate cement reinforced by strontium nitrate nanoparticles: fabrication and FEM analysis. Arab J Sci Eng 2023. https://doi.org/10.1007/s13369-023-08050-x.
[18] Raki E, Afrand M, Ali A. Influence of magnetic field on boiling heat transfer coefficient of a magnetic nanofluid consisting of cobalt oxide anddeionized water in nucleate regime: an experimental study. Int J Heat Mass Transf 2021;165:120669. Part A.
[19] Liu X, Adibi M, Shahgholi M, Tlili I, Mohammad Sajadi S, Abdollahi A, Li Z, Karimipour A. Phase change process in a porous Carbon-Paraffin matrix with different volume fractions of copper oxide Nanoparticles: a molecular dynamics study. J Mol Liq 2022;366:120296. https://doi.org/10.1016/j.molliq.2022.120296. ISSN 0167-7322.
[20] Li Z, Shahrajabian H, Bagherzadeh SA, Hamid J, Karimipour A, Tlili I. Effects of nano-clay content, foaming temperature and foaming time on density and cell size of PVC matrix foam by presented Least Absolute Shrinkage and Selection Operator statistical regression via suitable experiments as a function of MMT content. Phys Stat Mech Appl 2020;537:12263.
[21] Huang M, Borzoei H, Abdollahi A, Li Z, Karimipour A. effect of concentration and sedimentation on boiling heat transfer coefficient of GNPs-SiO2/deionized water hybrid Nanofluid: an experimental investigation. Int Commun Heat Mass Transf 2021;122:105141. https://doi.org/10.1016/j.icheatmasstransfer.2021.105141. ISSN 0735-1933.
[22] Almitani KH, Abu-Hamdeh NH, Etedali S, Ali A, Goldanlou AS, Golmohammadzadeh A. Effects of surfactant on thermal conductivity of aqueous silica nanofluids. J Mol Liq 2021;327:114883.
[23] Saad Kamel M, Lezsovits F, Ali A, Izadi M. Amelioration of pool boiling thermal performance in case of using a new hybrid nanofluid. Case Stud Therm Eng 2021;24:100872.
[24] A. Babaie, M. Rezaei, and R.L.M. Sofla, "Investigation of the effects of polycaprolactone molecular weight and graphene content on crystallinity, mechanical properties and shape memory behavior of polyurethane/graphene nanocomposites," vol. 96, pp. 53–68, 2019.
[25] A. Boudjellal et al., "A facile preparation strategy and characterization of polymer composite-based on polycaprolactone and alfa fibers/graphene nanoplatelets hybrids," vol. 337, p. 133940, 2023.
[26] I.S. Stefanović et al., "The impact of the polycaprolactone content on the properties of polyurethane networks," vol. 35, p. 105721, 2023.
[27] E. Shahsavari, I. Ghasemi, M. Karrabi, and H. Azizi, "Starch/polycaprolactone/graphene nanocomposites: shape memory behavior," vol. 32, no. 6, pp. 763–72, 2023.
[28] J. Wang, X. Lin, R. Wang, Y. Lu, and L. Zhang, "Self-healing, photothermal-responsive, and shape memory polyurethanes for enhanced mechanical properties of 3D/4D printed objects," vol. 33, no. 15, p. 2211579, 2023.
[29] B. Cetiner, G. Sahin Dundar, Y. Yusufoglu, and B. Saner Okan, "Sustainable engineered design and scalable manufacturing of upcycled graphene reinforced polylactic acid/polyurethane blend composites having shape memory behavior," vol. 15, no. 5, p. 1085, 2023.
[30] G. Liang et al., "Improvement of mechanical properties and solvent resistance of polyurethane coating by chemical grafting of graphene oxide," vol. 15, no. 4, p. 882, 2023.
[31] Badar MS, Shamsi S, Ahmed J, Alam MA. MD simulations: concept, methods, and applications. In: Transdisciplinarity. Springer; 2022. p. 131–51.
[32] W.F. Van Gunsteren and H.J. Berendsen, "Computer simulation of molecular dynamics: methodology, applications, and perspectives in chemistry," vol. 29, no. 9, pp. 992–1023, 1990.
[33] B. Leimkuhler and C. Matthews, "Molecular dynamics," vol. 39, p. 443, 2015.
[34] S.A. Hollingsworth and R.O. Dror, "Molecular dynamics simulation for all," vol. 99, no. 6, pp. 1129–43, 2018.
[35] A.P. Thompson et al., "LAMMPS-a flexible simulation tool for particle-based materials modeling at the atomic, meso, and continuum scales," vol. 271, p. 108171, 2022.
[36] K. Vollmayr-Lee, "Introduction to molecular dynamics simulations," vol. 88, no. 5, pp. 401–22, 2020.
[37] Rapaport DC. The art of molecular dynamics simulation. Cambridge university press; 2004.
[38] M.A. González, "Force fields and molecular dynamics simulations," vol. 12, pp. 169–200, 2011.
[39] S. Riniker, "Fixed-charge atomistic force fields for molecular dynamics simulations in the condensed phase: an overview," vol. 58, no. 3, pp. 565–78, 2018.
[40] Oluwajobi A, Chen X. The effect of interatomic potentials on the molecular dynamics simulation of nanometric machining. Int J Autom Comput 2011;8(3):326.
[41] Solms NV, O'Lenick R, Chiew Y. Leonard-Jones chain mixtures: variational theory and Monte Carlo simulation results. Mol Phys 1999;96(1):15–29.
[42] H.J. Berendsen, J.R. Grigera, and T.P. Straatsma, "The missing term in effective pair potentials," vol. 91, no. 24, pp. 6269–71, 1987.
[43] A.K. Rappé, C.J. Casewit, K. Colwell, W.A. Goddard III, and W.M. Skiff, "UFF, a full periodic table force field for molecular mechanics and molecular dynamics simulations," vol. 114, no. 25, pp. 10024–35, 1992.
[44] Huray PG. Maxwell's equations. John Wiley & Sons; 2011.
[45] Sarkar S, Selvam RP. Molecular dynamics simulation of effective thermal conductivity and study of enhanced thermal transport mechanism in nanofluids. J Appl Phys 2007;102(7):074302. 2007/10/01.
[46] D. McQuarrie, "Statistical mechanics university science books," pp. 222–3, 2000.